Journal of Applied Electrochemistry **31**: 793–798, 2001.

Synthesis and characterization of carbon-supported Pt–Ru–WO_x catalysts by spectroscopic and diffraction methods[†]

C. ROTH[1], M. GOETZ[2] and H. FUESS[1]
[1]*Institute for Materials Science, Darmstadt University of Technology, Petersenstrasse 23, D-64287 Darmstadt, Germany*
[2]*Institute of Chemical Technology, Darmstadt University of Technology, Petersenstrasse 20, D-64287 Darmstadt, Germany*

Received 18 January 2000; accepted in revised form 10 January 2001

Key words: electrocatalysis, fuel cells, nanoparticles, Pt, Pt–Ru, XPS

Abstract

Carbon-supported Pt–Ru–WO_x/C catalysts for application in PEMFC anodes were synthesized by a modified Bönnemann method. Their electrocatalytic activity for the oxidation of H_2/CO mixtures and CH_3OH was measured by *E*/*i*-curves in PEM single cell arrangements under working conditions. Information about composition, microstructure and nanomorphology was obtained by X-ray diffraction (XRD), X-ray photoelectron spectroscopy (XPS), X-ray fluorescence analysis (XFA) and transmission electron microscopy (TEM). X-ray diffraction data at room temperature show only one single Pt f.c.c. phase; no evidence of Ru, W and their oxides, respectively, is found. Hence, the presence of W and Ru as amorphous oxide species seems likely. Surface-sensitive XPS measurements detect Pt^0, platinum oxide and hydroxide species, metallic Ru, ruthenium oxide, hydrous ruthenium oxide and WO_3. For the crystalline platinum phase particle sizes of less than 2 nm were determined by TEM images and XRD patterns via solving the Scherrer equation. Temperature-dependent XRD measurements were performed to show the influence of ageing on the catalyst structure.

1. Introduction

Recently, liquid or vapour-feed direct methanol fuel cells (DMFCs) have gained increasing importance for application in transportation systems and mobile units. These cells offer solutions for environmental problems and offer advantages compared to fuel cells with indirect methanol supply.

State-of-the-art catalyst for the cathode compartment is a carbon-supported platinum powder whereas Pt–Ru/C alloys are used as the anode. Addition of ruthenium prevents the poisoning of the active platinum sites by carbon monoxide through oxidation of the CO-adsorbates. Intensive research by Gasteiger et al. [1] resulted in an optimum bulk stoichiometry of Pt:Ru 50:50 for the CO electrooxidation on well-characterized alloy surfaces at room temperature. Temperature-dependent investigations of the methanol electrooxidation at Pt–Ru bulk electrodes [2] and model systems [3] gave an optimum surface stoichiometry between 10 at % Ru at room temperature up to 40 at % Ru at 60 °C. Further testing of other (transition) metals revealed cocatalytic effects in the systems Pt–W [4], Pt–Mo [5], Pt–Sn [6] and Pt–Pb [7] but none of these binary systems shows an activity as high as the standard Pt–Ru/C. Investigations on ternary and quarternary catalyst formulations mainly focused on W, Mo, Sn [8], Os and Os–Ir [9] as additional third (fourth) element, and recently on transition metal phthalocyanines and porphyrines [10, 11] already tested for cathode purposes years ago. But despite some encouraging results a more exploratory approach does not seem to lead to real progress in catalyst research.

To investigate electrocatalytic activities, rotating disc experiments, CO-stripping voltammetry and PEM single cell arrangements belong to the well-known routine techniques in catalyst research. In contrast to this, characterization of the microstructure by physicochemical methods seems to be relatively scarce [12, 13], but necessary. Systematic investigation of the synergistic effects observed and intensive characterization of the most promising systems are a more convincing route to explain and predict increased catalytic activity.

In the present work Pt–Ru–WO_x/C catalysts of different stoichiometry were synthesized by a method developed by Bönnemann and coworkers [14] and characterized by X-ray powder diffraction (XRD), X-ray photoelectron spectroscopy (XPS), X-ray fluorescence analysis (XFA), transmission electron microscopy

[†] Paper presented at the workshop on "Electrocatalysis in direct and indirect methanol fuel cells" held at Portoroz, Slovenia, September 1999.

(TEM) and electrochemical single cell measurements using H_2/CO mixtures and CH_3OH. Detailed electrochemical investigations on similar binary alloy colloids were previously carried out by Schmidt et al. [15, 16] in collaboration with the Bönnemann group. Their stripping voltammetry results and rotating disk measurements demonstrate the high electrocatalytic activity of those colloidal catalysts for CO and CO/H_2 electrooxidation, respectively. The aim of the present investigations is to obtain further information on the composition, microstructure and nanomorphology in the ternary Pt–Ru–WO_x/C colloid system by combination of spectroscopic and diffraction methods and comparison of the results.

2. Experimental details

2.1. *Syntheses*

Carbon black (Vulcan XC-72, Cabot Intern.) with a specific surface area (BET) of 290 $m^2\ g^{-1}$ was used as support for all catalysts. According to a slightly modified method, originally developed by Bönnemann et al. (1991), the carbon-supported Pt–Ru–WO_x catalysts were synthesized in a dry nitrogen atmosphere using dry solvents (tetrahydrofurane) and nonhydrated salts ($PtCl_2$, $RuCl_3$, WCl_6, tetraoctylammoniumbromide). Modifications of the synthesis were published by Götz and Wendt [17].

2.2. *Characterization by XRD, XPS, XFA and TEM*

The catalysts were investigated by X-ray powder diffraction using a STOE STADI-P, with germanium monochromatized CuK_α radiation and a position-sensitive detector with 40° aperture in transmission mode. Temperature-dependent measurements in the temperature range 100–600–100 °C, 10 °C min^{-1} heating rate and 3 min holding time under nitrogen flow were realized by a STOE diffractometer with CuK_α radiation.

The XPS measurements were carried out on a PHI 5700 MultiTechnique ESCA (Perkin Elmer) with AlK_α radiation at a power of 300 W. A suitable pass energy of 11.75 eV was chosen, while a pressure of 3×10^{-8} mbar was maintained within the spectrometer chamber. Samples were prepared by pressing a small amount of the supported catalyst powder into In foils. The spectra were fitted and evaluated by the standard software Igor Pro (Wavemetrics Inc., Oregon, 1988) using a mixed Gauss–Lorentzian function [18].

Metal loading and composition of the supported catalysts were measured using a Xlab 2000 (Spectro analytical instruments GmbH). Specific calibration was realized by measuring a series of metal oxides on carbon as oxygen, in contrast to chloride, gives no contribution to spectral noise.

A Jeol TEM 3010 with an acceleration voltage of 300 kV and LaB_6 cathode was applied for high resolution images of the supported catalysts. Samples were prepared by suspending the catalyst powder in alcohol and depositing a drop of the suspension on a standard copper grid covered with carbon.

2.3. *Electrochemical investigation*

The electrocatalytic activity of the synthesized catalysts was measured in PEM single cell arrangements at a temperature of 75 °C for H_2/CO and 95 °C for methanol operation, respectively. Membrane electrode assemblies (MEA) with an active electrode area of 25 cm^2 were manufactured by a spraying technique originally developed by Gottesfeld et al. [19] and mounted in a commercially available graphite cell block. A platinum loading of 0.4 mg cm^{-2} per electrode was applied using a standard Pt catalyst (E-TEK) at the cathode and Nafion© 117 (DuPont) as proton conducting membrane. Current voltage curves were recorded after 14 days of continuous cell operation with pure oxygen as cathode feed gas in both cases.

3. Results and discussion

3.1. *X-ray fluorescence analysis*

The results of the analysis show that the stoichiometry quantities employed for catalyst synthesis are in good agreement with the measured stoichiometry in XFA (Table 1). The platinum and ruthenium metal loading is permanently kept at 20 wt %, whereas the total metal loading increases due to the amount of tungsten added. Constant Pt and Ru metal loading should allow a comparison of the electrocatalytic activity between catalysts of varying tungsten stoichiometry.

The metal loading of commercially available 20 wt % Pt, 20 wt % Ru, 20 wt % Pt–Ru (1:1) on Vulcan XC-72 catalysts are of varying quality, sometimes not providing

Table 1. Stoichiometry and metal loading of different carbon-supported catalysts

Sample	Total metal loading /wt %	Pt/Ru metal loading /wt %	Pt /wt %	Ru /wt %	W /wt %
(1:1:1.5)	39	21	14	7	18
(1:1:2)	51	22	15	7	29
Pt (E-TEK)	19		19	–	–
Ru (E-TEK)	12		–	12	–
Pt–Ru (E-TEK)	15	15	10	5	–

the amount of catalytic active material guaranteed in the specification. Nevertheless the 1:1 stoichiometry of the binary catalyst checked agreed within experimental error.

3.2. *Transmission electron microscopy*

Figure 1 shows nanocrystals with particle sizes of 1–2 nm for the Pt–Ru–WO_x/C (1:1:1.5) catalyst, homogeneously dispersed on the edges of each micrometer-sized carbon support grain. Samples of different composition do not differ in appearance, therefore only images of the Pt–Ru–WO_x/C (1:1:1.5) catalyst are presented here. In HRTEM (Figure 2) the lattice planes of the nanoparticles are displayed, thus giving evidence of their crystallinity. Although lattice planes of individual particles were clearly resolved, the corresponding d values were not determined as, in small particles, distortion of the lattice planes occurs [20, 21]. Additional electron

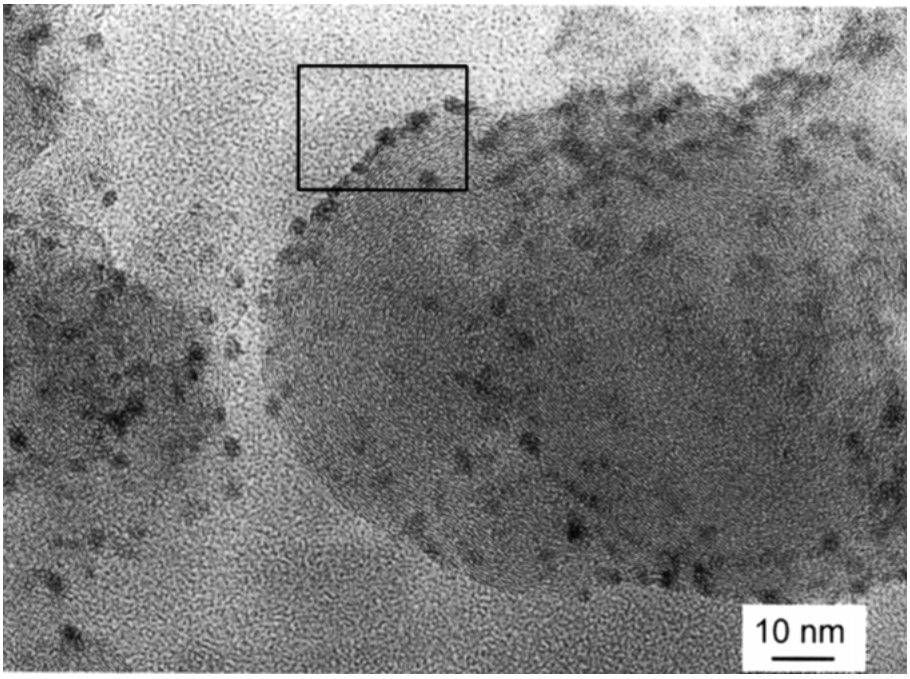

Fig. 1. TEM image of Pt–Ru–WO_x/C (1:1:1.5).

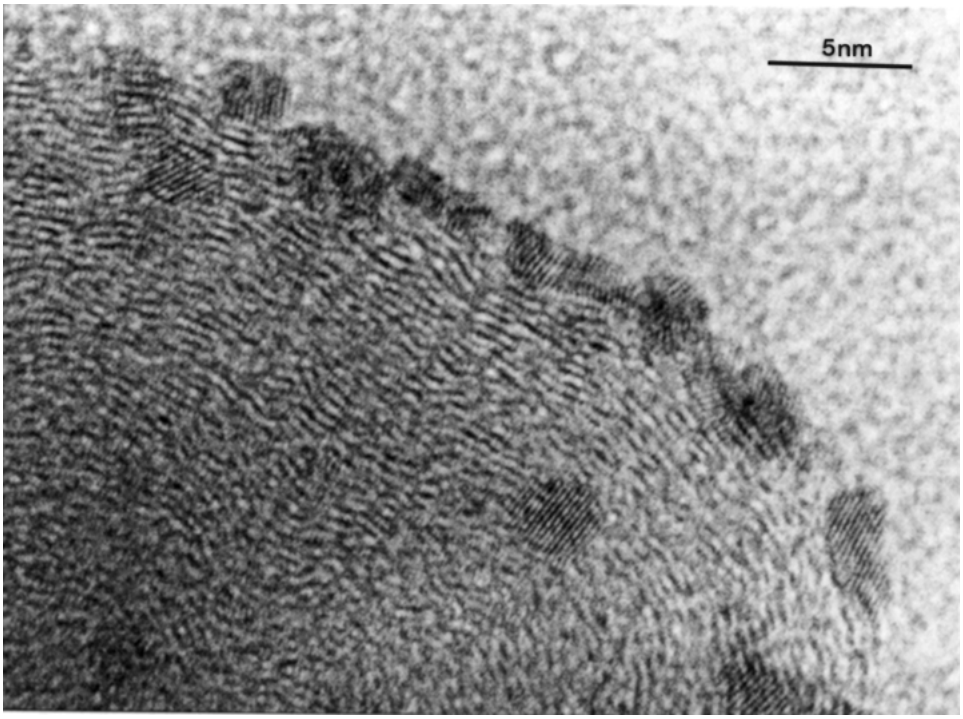

Fig. 2. HRTEM image of Pt–Ru–WO_x/C (1:1:1.5).

energy loss spectra (EELS) on specific grains will be performed in order to determine the elemental composition of the cluster. Mapping the oxygen distribution of the catalyst powder may indicate where the amorphous tungsten species are located.

3.3. *X-ray photoelectron spectroscopy*

XPS is used to define the oxidation states of the catalytic and cocatalytic acting metals in the catalyst powder. Although XPS is a surface-sensitive method, in the case of supported nanoparticles the assumption of obtaining bulk information can be made, since most of the cluster atoms are surface atoms. The obviously asymmetric-shaped Pt4f and Ru3p signals were fitted with a mixed Gauss–Lorentzian function. The Pt4f signal (Figure 3) could be resolved into three doublets; the most intense peak at 71.4 eV being attributed to metallic Pt, the less prominent doublet at BE 0.8 eV higher than Pt^0 being assigned to Pt(+II) with a BE comparable to that of Pt in $Pt(OH)_2$, while the third doublet at 73.6 eV seems likely to be some kind of surface oxide. The Pt^0 peak is slightly shifted to higher binding energies in accordance with the small particle sizes, as reported by Franke et al. [22]. In the case of the ruthenium the Ru3p signal was deconvoluted into three distinguishable peak pairs of different intensity at BE 462.0, 462.4 and 463.8 eV. The Ru3p signal was chosen, as the Ru3d peak strongly overlaps with the C1s signal of the carbon support. The doublet at BE 462.0 eV was attributed to Ru^0, while the two signals at higher BE were assigned to RuO_2 (BE 462.4 eV) and hydrous RuO_2 (BE 463.8 eV), as hydrous oxide species shift to higher BE in comparison to non-hydrous ones, even if the oxidation states are equal [23, 24]. Because of the poor statistics of the Ru3p signal quantitative analyses were not carried out. Tungsten appears as WO_3 in all Pt–Ru–WO_x/C catalysts checked. Survey spectra of catalysts with different composition are very similar, differing only in the peak intensities.

3.4. *X-ray powder diffraction*

XRD investigations were carried out on the as-synthesized Pt–Ru–WO_x/C catalysts at room-temperature (Figure 4) and in a temperature cycle 100–600–100 °C (Figure 5). Despite different tungsten contents the pow-

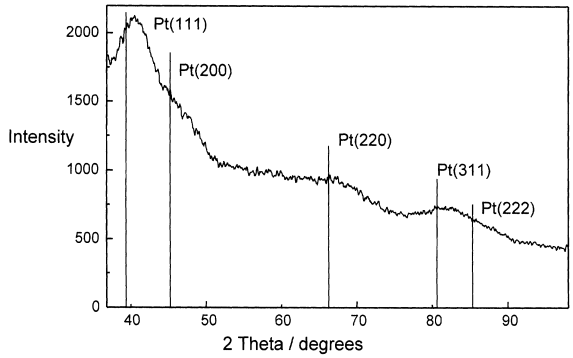

Fig. 4. Powder pattern as-synthesized (1:1:1.5) catalyst.

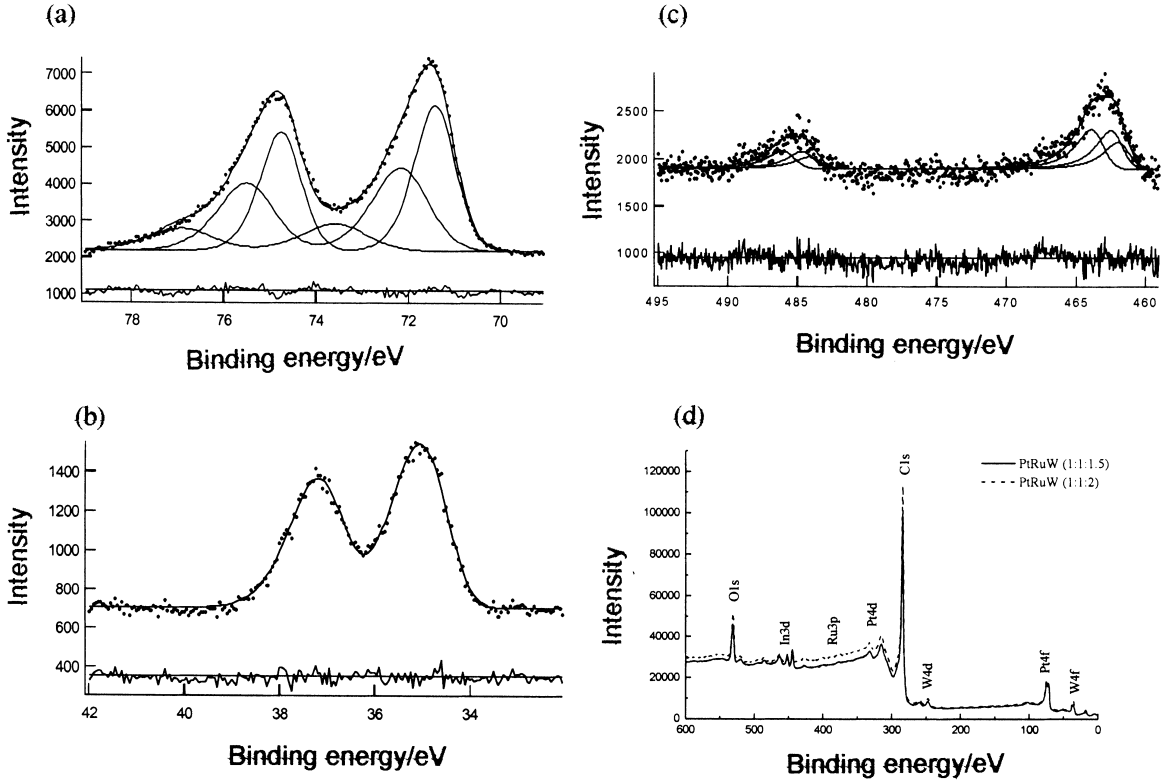

Fig. 3. Evaluation of the X-ray photoelectron spectra. (a) Deconvolution of the Pt4f signal; (b) deconvolution of the Ru3p signal; (c) fit of the W4f signal; and (d) survey spectra of Pt–Ru–WO_x/C (1:1:1.5) and Pt–Ru–WO_x/C (1:1:2) catalyst.

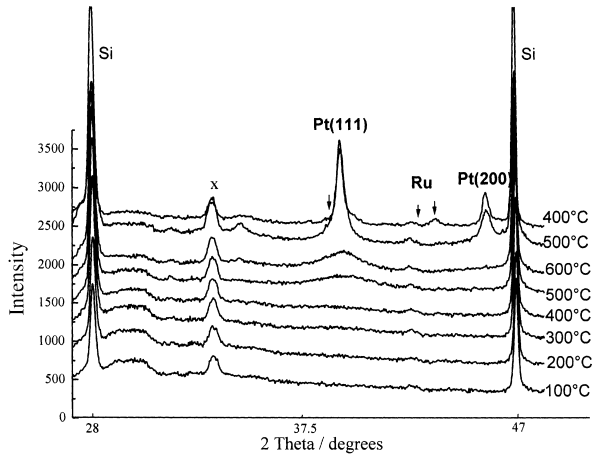

Fig. 5. Powder pattern annealed (1:1:1.5) catalyst. x = support.

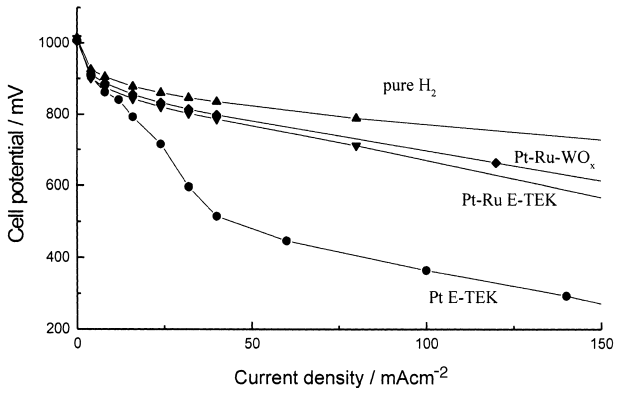

Fig. 6. Electrocatalytic activity of Pt–Ru–WO_x/C (1:1:1) compared to carbon-supported Pt and Pt–Ru E-TEK, H_2/150 ppm CO, T = 75 °C, 0.4 mg cm^{-2} platinum.

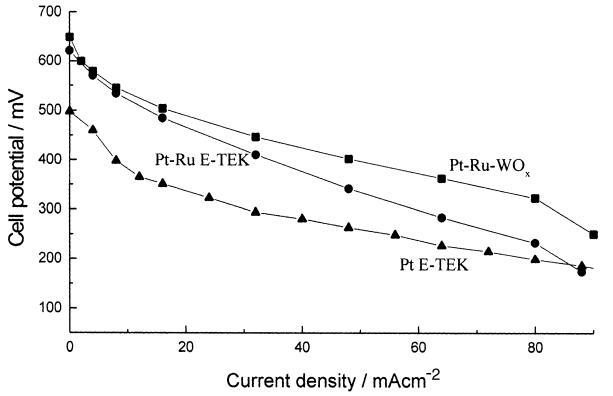

Fig. 7. Electrocatalytic activity of Pt–Ru–WO_x/C (1:1:1) compared to carbon-supported Pt and Pt–Ru E-TEK, CH_3OH (1 M aqueous solution), T = 95 °C, 0.4 mg cm^{-2} platinum.

der patterns of the as-synthesized catalysts look alike, exhibiting the characteristic reflections of the platinum f.c.c structure. A shift to higher 2Θ values indicating the partial substitution of Pt atoms by ruthenium, as observed by Gurau et al. [9] and Arico et al. [12], was not taken into account as contraction or dilatation of the lattice planes frequently occurring in small particles will make a correct evaluation of the d values impossible. Therefore Vegard's law was not applied to determine the amount of Ru in a possible Pt–Ru alloy. No evidence of reflections related to Ru, RuO_2, W or WO_3 phases was found in the range 2Θ 30–90° (Figure 4). Using CuK_α radiation the most intense oxide reflections should appear at 28.1° 2Θ for RuO_2(1 1 0), 35.5° for RuO_2(1 0 1) and 24.4° for WO_3(2 0 0), respectively, but a huge carbon support peak overlaps at low angles preventing the detection of any reflections in the range $2\Theta < 30°$.

During the following heating process the mean platinum particle size, determined by the Scherrer equation [25], increased from less than 2 nm in the as-synthesized state up to 20 nm in the annealed catalyst (platinum (1 1 1) reflection). After the first cooling step down to 500 °C Ru reflections occurred that grew further despite decreasing temperature. Static 16 h ageing measurements at 350 °C in nitrogen atmosphere resulted in distinct Ru reflections, stressing the fact that further investigation of static and dynamic ageing might be helpful in catalyst research.

3.5. *Electrochemical investigation*

Current potential curves obtained after 14 days continuous cell operation are presented in Figure 6. In comparison to the results of the Pt–Ru–WO_x/C catalyst E/i-curves of a commercially available Pt/C and Pt–Ru/C catalyst purchased by E-TEK inc. are shown. The ternary Pt–Ru–WO_x/C (1:1:1) catalyst shows a 15% better performance at a typical working potential of 600 mV in H_2/150 ppm CO operation than the Pt–Ru/C standard. In Figure 7 results of the same sample operated with vaporized methanol (1 M aqueous solution) at 95 °C are shown in comparison with Pt/C and Pt–Ru/C E-TEK. At a working potential of 400 mV a 40% increase in activity is found compared to the standard carbon-supported Pt–Ru catalyst.

4. Conclusions

It was shown by X-ray powder diffraction and transmission electron microscopy that the Bönnemann synthesis leads to homogeneously dispersed nanocrystals with an average particle size of 1–2 nm. Powder patterns of the carbon-supported catalysts exhibit the characteristic reflections of the platinum f.c.c structure according to the ICDD data base. Reflections of tungsten, ruthenium and their oxides, respectively, are not found, hence the presence of W and Ru as amorphous oxide species seems likely. In accordance with these results surface-sensitive XPS measurements give evidence of metallic platinum, platinum hydroxide and surface oxide species, ruthenium, hydrous and nonhydrous RuO_2 and WO_3. Further investigations by EELS and XAS should help to settle unsolved questions about the

structure and nanomorphology of carbon-supported fuel cell catalysts.

Acknowledgement

The authors are grateful to Prof. Wendt for helpful discussions. Support of this work by the Deutsche Forschungsgemeinschaft and Fonds der Chemischen Industrie is gratefully acknowledged. Thanks are due to B. Krause, J. Fritsche and G. Miehe.

References

1. H.A. Gasteiger, N. Markovic, P.N. Ross and E.J. Cairns, *J. Phys. Chem.* **98**(2) (1994) 617.
2. H.A. Gasteiger, N. Markovic, P.N. Ross and E.J. Cairns, *J. Electrochem. Soc.* **141**(7) (1994) 1795.
3. T. Iwasita, H. Hoster, A. John-Annacker, W.F. Lin and W. Vielstich, *Langmuir* **16** (2000) 522.
4. P.K. Shen and A.C.C. Tseung, *J. Electrochem. Soc.* **141** (1994) 3082.
5. J.A. Shropshire, *J. Electrochem. Soc.* **112** (1965) 465.
6. M.M.P. Janssen and J. Moolhuysen, *Electrochim. Acta* **21** (1976) 861.
7. B. Beden, F. Kardigan, C. Lamy and J.M. Leger, *J. Electroanal. Chem.* **127** (1981) 75.
8. M. Götz and H. Wendt, *Electrochem. Soc. Proc.* **98**(27) (1999) 291.
9. B. Gurau, R. Viswanathan, R. Liu, T.J. Lafrenz, K.L. Ley, E.S. Smotkin, E. Reddington, A. Sapienza, B.C. Chan, T.E. Mallouk, S. Sarangapani, *J. Phys. Chem. B* **102** (1998) 9997.
10. J.S. Bett, H.R. Kunz, A.J. Jr. Aldykiewicz, J.M. Fenton, W.F. Bailey, D.V. McGrath, *Electrochim. Acta* **43**(24) (1998) 3645.
11. J.F. van Baar, J.A.R. van Veen, N. de Wit, *Electrochim. Acta* **27**(9) (1982) 1315.
12. A.S. Arico, P. Creti, H. Kim, R. Mantegna, N. Giordano and V. Antonucci, *J. Electrochem. Soc.* **143**(12) (1996) 3950.
13. S. Mukerjee and J. McBreen, *J. Electroanal. Chem.* 448 (1998) 163.
14. H. Bönnemann, W. Brijoux, R. Brinkmann, E. Dinjus, T. Joussen and B. Korall, *Angew. Chem. Int. Ed. Engl.* **30** (1991) 1312.
15. T.J. Schimdt, M. Noeske, H.A. Gasteiger, R.J. Behm, P. Britz, W. Brijoux and H. Bönnemann, *Langmuir* **13**(10) (1997) 2591.
16. T.J. Schimdt, H.A. Gasteiger and R.J. Behm, *J. New Mat. Electrochem. Systems* **2** (1999) 27.
17. M. Götz and H. Wendt, *Electrochim. Acta* **43**(24) (1998) 3637.
18. I. Kojima and M. Kurahashi, *J. Electr. Spectr. Rel. Phen.* **42** (1987) 177.
19. M.S. Wilson and S. Gottesfeld, *J. Electrochem. Soc.* **139** (1992) L28.
20. C. Solliard and M. Flüeli, *Surf. Sci.* **156** (1985) 487.
21. M. Ya. Gamarnik, *Phys. Stat. Sol. B* **164** (1991) 107.
22. R. Franke, PhD thesis (1999).
23. D.R. Rolinson, P.L. Hagans, K.E. Swider, J.W. Long, *Langmuir* **15** (1999) 774.
24. J.F. Moulder, W.F. Stickle, P.E. Sobol and K.D. Bomben, *in* J. Chastain and R.C. King Jr (Ed.), 'Handbook of X-ray Photoelectron Spectroscopy', (1992).
25. M.M.A. Guerin and A.G. Alvarez, *Cryst. Rev.* **4** (1995) 261.